Environmental Pollution 270 (2021) 116228

Contents lists available at ScienceDirect

Environmental Pollution

journal homepage: www.elsevier.com/locate/envpol

Exploring the external exposome using wearable passive samplers - The China BAPE study☆

Jeremy P. Koelmel [a], Elizabeth Z. Lin [a], Pengfei Guo [a], Jieqiong Zhou [a], Jucong He [a], Alex Chen [b], Ying Gao [c], Fuchang Deng [c], Haoran Dong [c], Yuanyuan Liu [c], Yu'e Cha [c], Jianlong Fang [c], Chris Beecher [d], Xiaoming Shi [c, e], Song Tang [c, e], Krystal J. Godri Pollitt [a, *]

[a] Department of Environmental Health Sciences, School of Public Health, Yale University, New Haven, CT, 06520, USA
[b] Department of Computer Science, Yale University, New Haven, CT, 06520, USA
[c] China CDC Key Laboratory of Environment and Population Health, National Institute of Environmental Health, Chinese Center for Disease Control and Prevention, Beijing, 100021, China
[d] IROA Technologies, Chapel Hill, NC, USA
[e] Center for Global Health, Nanjing Medical University, Nanjing, Jiangsu, 211166, China

ARTICLE INFO

Article history:
Received 29 June 2020
Received in revised form
2 December 2020
Accepted 3 December 2020
Available online 6 December 2020

Keywords:
personal exposure monitoring
Exposomics
Passive sampling
Mass spectrometry
Non-negative matrix factorization
Pollutants

ABSTRACT

Environmental exposures are one of the greatest threats to human health, yet we lack tools to answer simple questions about our exposures: what are our personal exposure profiles and how do they change overtime (external exposome), how toxic are these chemicals, and what are the sources of these exposures? To capture variation in personal exposures to airborne chemicals in the gas and particulate phases and identify exposures which pose the greatest health risk, wearable exposure monitors can be deployed. In this study, we deployed passive air sampler wristbands with 84 healthy participants (aged 60–69 years) as part of the Biomarkers for Air Pollutants Exposure (China BAPE) study. Participants wore the wristband samplers for 3 days each month for five consecutive months. Passive samplers were analyzed using a novel gas chromatography high resolution mass spectrometry data-processing workflow to overcome the bottleneck of processing large datasets and improve confidence in the resulting identified features. The toxicity of chemicals observed frequently in personal exposures were predicted to identify exposures of potential concern via inhalation route or other routes of airborne contaminant exposure. Three exposures were highlighted based on elevated toxicity: dichlorvos from insecticides (mosquito/malaria control), naphthalene partly from mothballs, and 183 polyaromatic hydrocarbons from multiple sources. Other exposures explored in this study are linked to diet and personal care products, cigarette smoke, sunscreen, and antimicrobial soaps. We highlight the potential for this workflow employing wearable passive samplers for prioritizing chemicals of concern at both the community and individual level, and characterizing sources of exposures for follow up interventions.

1. Introduction

Environmental factors are the leading contributors to certain diseases (Wheelock and Rappaport, 2020; Rappaport, 2016; Prüss-Üstünet al., 2016) and many of these environmental risks can be mediated: according to the 2017 WHO report on the estimation of the global burden of diseases (GBD) attributable to unhealthy environments, 23% of global deaths result from modifiable environmental risk factors (Prüss-Üstünet al., 2016). To prioritize and reduce the exposure to environmental contaminants of concern, techniques for comprehensive characterization of environmental exposures are needed. These techniques fall under the field of exposomics where the totality of environmental exposures throughout an individual's life course are measured (Wild, 2005).

Recently, wearable personal passive samplers were developed to accommodate the needs of exposomic studies in airborne organic nonpolar pollutants (Wanget al., 2019a; O'Connell et al., 2014; Lin et al., 2020; Hammel et al., 2018; Hammel et al., 2016). These passive samplers are noninvasive, lightweight and low cost, allowing people from all age groups to wear the passive samplers in

☆ This paper has been recommended for acceptance by Payam Dadvand.

* Corresponding author. Department of Environmental Health Sciences, Yale School of Public Health, 60 College Street, Room 523, New Haven, CT, 06510, USA.
E-mail address: krystal.pollitt@yale.edu (K.J. Godri Pollitt).

https://doi.org/10.1016/j.envpol.2020.116228
0269-7491/

order to capture the chemical profile from multiple microenvironments over a complete or critical exposure window (e.g. exposure during pregnancy or neonatal exposure) in life. Samplers can then be analyzed by high-resolution mass spectrometry for targeted, suspect screening, or non-targeted analysis. The FreshAir wristband (Lin et al., 2020) was developed with a unique design which removes variance unrelated to airborne concentrations of chemicals. Different from other passive samplers, its sheltered design minimizes the effects of surface air flow that influences uptake rates (Zhanget al., 2013; Seethapathy et al., 2008) and direct contact with the skin and cosmetic products. Therefore, monitored levels more closely resemble the inhalation exposure route.

Coupling the FreshAir wristband with gas chromatography high-resolution mass spectrometry (GC-HRMS) suspect screening (Aksenovet al., 2020), thousands to tens-of-thousands of known unknowns and unknown unknowns can be annotated or classified. Because of the computational requirements to process these massive mass spectrometry datasets (gigabytes to terabytes), new algorithms are needed to enable the processing of data from large cohort studies (Aksenovet al., 2020). We therefore introduce a modular workflow combining vendor or open source deconvolution and identification algorithms on pooled or representative samples (computational intensive step) with targeted peak detection across all samples (computationally inexpensive step) to increase throughput and enable large cohort studies. This workflow is applied to personal exposure monitoring implementing FreshAir wristbands in a large cohort of Chinese healthy elderly as part of the Biomarkers for Air Pollutants Exposure (China BAPE) study.

In this study we aim to understand pollutant exposure to a high-risk population. China has a high percentage of disease burden that can be minimized through environmental improvements (Prüss-Üstünet al., 2016). For example, in Taiyun, China, it was estimated that 2.4–4.9% of the cities GDP was spent on health damages caused by ambient particulate matter exposure, and infrastructure changes and transition to cleaner fuels could save between 200 and 1100 lives for the city in a scenario for 2010 (Zhanget al., 2010). In addition, the impacts of environmental factors are disproportionately distributed across age; except for children under five, adults aged from 50 to 75 are the most vulnerable populations with increased risks of non-communicable diseases (Breysseet al., 2010; Guan et al., 2016; Choi et al., 2017). Using the personal exposure sampler, we were able to determine compounds of greatest concern for this vulnerable adult population including insecticides, chemicals from household products, and exposures from combustion. Previous studies evaluating the health effects of air pollution have mostly focused on ambient particulate matter, often capturing only the bulk mass concentration of exposure; chemical constituents of particulate matter are well recognized to influence the toxicity of these inhaled airborne contaminants (Cassee et al., 2013; Kelly and Fussell, 2012(Gao et al., 2020)). Moreover, focus on exclusively particulate matter excludes consideration to environmental chemicals in the gas phase which contribute to the diverse mixture of exposures. We demonstrate variation in chemical exposures based on behavior and changing weather across months. In addition to providing information on environmental contaminants on the population level, using passive samplers we also monitored exposures to chemicals associated with personal behaviors, cultural traditions, and social behaviors on the individual level (e.g. indoor pesticide use and cooking ingredients).

2. Material and methods

2.1. Study population and study design

Eighty-four healthy adult participants (60–69 years) were recruited as part of the China BAPE Study from the Dianliu community (28,025 residents) in Jinan, a major city in the Beijing-Tianjin-Hebei region. The study protocol has been reviewed and approved by the Ethics Review Committee of National Institute of Environmental Health (NIEH), Chinese Center for Disease Control and Prevention (China CDC, No. 201816). Written informed consent was obtained from each study participant. Details of participant enrollment and the design of the China BAPE Study have been previously described in Tang et al. (2020). Inclusion criteria, questionnaire details, and sample collection times are provided in the Supplemental Information and Figure S1; for the subset of participants (66/84) who filled out questionnaires details are provided in Table 1. Briefly, participants took part in a comprehensive 3-day exposure assessment each month for five consecutive months from September 10th, 2018 to January 19th, 2019. To accommodate study team logistics, participants were subdivided into three groups and the exposure assessment period of each group was staggered through each month. Each exposure assessment period was three days and were evenly distributed in the 2nd and 3rd week of each month as shown in Figure S1. A member of the study team visited each participants' house at the start (Day 1) and end (Day 3) of this assessment period. The start and end days were the same for all 25–26 participants in each assessment group. Participants were given a passive air pollutant sampler in the form of a wristband to continuous wear over these three days. The wristband was only removed while bathing or sleeping. Participants were asked to place the wristband on a bedside table overnight. Not all participants returned for all 5 months, and a total of 298 personal exposure profiles (3-day averages) were obtained across the 84 participants. No participants lived in the same household. At the end of each month's exposure assessment period, a member of the study team collected the wristband sample from participants' home and stored the wristband samples at −80 °C until analysis. In addition to collecting personal exposure samples, similar passive air samplers were deployed outdoors at the top floor of Ankang Community Hospital in Dianliu community. Passive samplers were

Table 1
Individual and household characteristics of study participants (N = 66/84).

Characteristic	N (%) or Mean ± SD
Gender	
Male	33 (50.0%)
Female	33 (50.0%)
Education level	
Below middle school	7 (10.6%)
Secondary school	45 (68.1%)
Bachelor and above	14 (21.2%)
Age (years)	65.1 ± 2.8
Income (10k yuan/year)	4.5 ± 3.7
BMI (kg/m^2)	24.9 ± 2.7
Floor level[a]	
1st-5th floor	50 (76.9%)
6th-33rd floor	15 (23.1%)
Housing type	
Apartment Complex	59 (89.3%)
Others	7 (10.7%)
Year of Home Construction[a]	
1977–1999	14 (29.8%)
2000–2016	33 (70.2%)
Distance from major road arteries (m)	
<50	20 (30.3%)
50–200	31 (46.9%)
>200	15 (22.7%)
Indoor Room Area (m^2)	79.4 ± 36.6

Note that participant characteristics were obtained for 66 of the 84 total participants, due to failure to return questionnaires for the remaining participants. SD stands for standard deviation.
[a] 1 missing in floor level, 19 missing in year of home construction.

deployed for three-days in parallel with each participant group for every month of the study (total of 15 samples).

Hourly means of ambient temperature were collected from a stationary ambient air monitoring station operated by the Jinan Environmental Monitoring Centre located 1.5 km from the Dianliu community and used in this study. Questionnaire details used in this study were hours of windows being open and closed in the household (Supplemental Information).

2.2. Reagents

Methanol and hexane (Optima LC/MS grade), toluene and dichloromethane (HPLC grade), and polydimethylsiloxane polymer were purchased from Fisher Scientific (Hampton, NH, USA). Analytical standards were greater than 98% purity, they were purchased from Accustandard (New Haven, CT, USA) and SPEX (Metuchen, NJ, USA).

2.2.1. Passive air wristband samplers

FreshAir Wristband/Clip: Personal inhalation exposure to contaminants was evaluated using a novel wearable passive air sampler known as the FreshAir wristband (Lin et al., 2020). This wristband consisted of a band that housed a polytetrafluoroethylene (PTFE) chamber (Fig. 1A). This PTFE chamber contained four custom fabricated PDMS sorbent bars which were used to passively absorb airborne chemicals (Fig. 1A). PDMS sorbent bars were custom fabricated and cleaned in a vacuum oven (2 h, 300 °C) under of 0.1–0.3 L/min flow of high purity nitrogen (99.99%) at Yale prior to use in the China BAPE Study. Cleaned PDMS sorbents were individually placed in microvial inserts and stored in air-tight 2 mL amber glass vials with PTFE septa caps. PDMS sorbent bars were shipped to the National Institute of Environmental Health (NIEH), Chinese Center for Disease Control and Prevention (China CDC). Immediately prior to deployment, a member of the study team positioned four cleaned PDMS sorbent bars into the PTFE chamber secured in place using pre-cleaned neodymium magnets (K&J Magnetic, Plumsteadville, PA, USA) and assembled the FreshAir wristband. The wristbands were worn by participants for the three-day exposure assessment period. A member of the study team returned the PDMS sorbent bars from the wristband back to the glass storage vials using stainless steel forceps immediately following the sampling period. Samples were stored at −80 °C in Beijing at the NIEH, China CDC and cold shipped to Yale for analysis.

Stationary passive samplers were also used in the form of

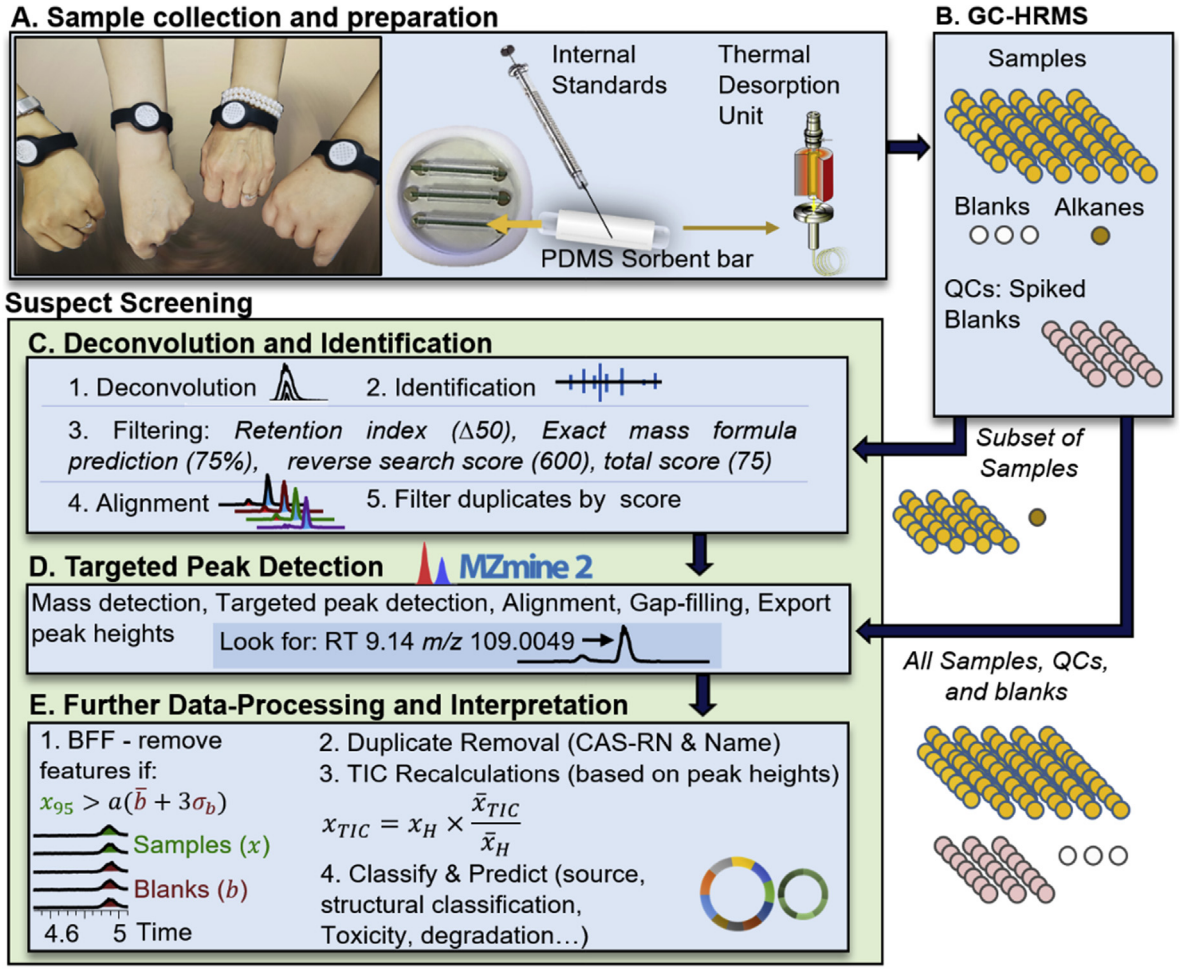

Fig. 1. Personal exposure monitoring gas chromatography high resolution mass spectrometry (GC-HRMS) workflow. These samplers consist of a silicone band which houses a PTFE chamber and contains three custom fabricated PDMS sorbent bars (A). Bars are spiked with labeled standards, and desorbed onto the GC-HRMS instrument (A). Data for samples, blanks, alkanes, and quality controls (QCs) are acquired (B). A subset of samples is deconvoluted and annotated using stringent filtering parameters for higher confidence identifications (C). The resulting aligned peak list containing retention times (RT) and mass to charge values (m/z) of features, is used for targeted peak detection across all samples and blanks (D) after which blank feature filtering (BFF) is applied to remove background signal (E), where $x_{95\%}$ = sample 95 percentile, $\bar{b}$ = blank average, σ_b = standard deviation of the blank.

FreshAir clips. These clips were similar to the FreshAir wristband design with the exception that the PTFE chamber was mounted in a magnetic clip. FreshAir clip were deployed at the top floor of Ankang Community Hospital during 3-day monitoring per visit in Dianliu community.

2.3. Gas chromatography high resolution mass spectrometry (GC-HRMS) acquisition and data-processing

Analytes were not predetermined. Any analyte in the nearly 800,000 chemicals within the NIST/Wiley library, which could be sorbed by the PDMS, extracted by thermal desorption, volatized in the GC-HRMS, and which had airborne concentrations sufficient for detection in this study could be detected.

2.3.1. PDMS bar preparation, sample introduction, and GC-HRMS acquisition

All laboratory glassware and tools were rinsed with methanol and baked at 75 °C for at least 24 h before use. All cleaned glassware and tools were stored at 75 °C oven until use. Following the sampling collection, PDMS sorbent bars were immediately removed by the study team from the housing chamber using stainless steel forceps and returned to sealed glass storage vials and stored at −80 °C. Immediately prior to analysis, PDMS sorbent bars were loaded with an internal standard mixture which contained 4,4′-dibromooctafluorobiphenyl, 5′-fluoro-2,3′,4,4′,5-pentabromodiphenyl ether, naphthalene-d8, 1-methylnaphthalene-d10, acenaphthene-d10, fluorene-d10, phenanthrene-d10, fluoranthene-d10, pyrene-d10, perylene-d12, phenol-d5, and p-terphenyl-d10. Sorbent bars were then placed into pre-cleaned glass autosampler tubes (Gerstel, Linthicum, MD, USA) on a temperature controlled autosampler tray maintained at 10 °C (MéCour, Groveland, MA, USA). For sample analysis, an autosampler tube was transferred into a thermal desorption unit (TDU; Gerstel, Linthicum, MD, USA). The TDU was initially held at 30 °C for 1.1 min and then ramped at 720 °C per minute to 280 °C (5 min hold) under a flow rate of 350 mL/min of helium gas (99.999%). Extracted analytes were cyro-focused to −90 °C on a 2 mm, glass wool deactivated liner in a cooled injection system (Gerstel, Linthicum, MD, USA) cooled to −90 °C. The transfer line between the TDU and cooled liner was maintained at 250 °C.

Analyses were directly transferred to the GC column (TG-5SILMS, 30 m × 0.25 mm x 0.25 μm; ThermoFisher, Waltham, MA, USA). The carrier gas flow (helium) was set to 1.4 mL/min and the GC oven was held at 70 °C for 1 min and then ramped at 7 °C/min to 300 °C. The final temperature was held for 4.0 min for a total runtime of 37.86 min. During the analysis, full-scan electron ionization (EI) mass spectra (m/z 53.4–800) was recorded at an acquisition rate of 4 Hz on a Q-Exactive Orbitrap mass spectrometer (ThermoFisher, Waltham, MA, USA).

QCs and blanks (laboratory and transport) were run every 5 samples. Due to the non-selective sampling nature of PDMS, coupled with the thermal desorption extraction method, a high concentration of chemicals was introduced onto the GC-HRMS. Therefore, samples were introduced in randomized batches, which were limited to a maximum of 80 acquisitions (samples, controls and standards). Batches were followed by a cleaning protocol which included the source.

The general sample preparation, GC-HRMS acquisition and data-processing workflow is shown in Fig. 1.

2.3.2. Deconvolution and identification

The Thermo Deconvolution Plugin was used for suspect screening. Alkanes were used to calculate an alkane retention index and compounds were searched against the following libraries: NIST 2017, WILEY Registry 11, and GC orbitrap specific (contaminants (2017) and PCBs) EI spectral libraries. Higher confidence was obtained for tentative identifications using the following filters (Fig. 1C; Step 3): retention index total maximum deviation: 50, and percent deviation: 1.5%; reverse search index greater than 600, reverse high-resolution filter greater than 75, and total score greater than 75. These filters were optimized using over 60 diverse pollutant standards, with the final filtering parameters providing the correct top-hit annotation for all standards (or a close isomer, for example with only a chlorine position changed) while minimizing the number of falsely identified background peaks. If no column was specified in the library, then the column was assumed to be the same column as used in our experiments. The high-resolution filter calculates the formula of fragments using only the atoms contained in the molecular formula, and higher scores indicate a higher portion of fragments which have exact masses which can be predicted using these atoms. Reverse searches indicate that only fragments from the library were considered in the scoring algorithm (reducing penalization from co-eluting compounds and background). For individual compounds which were discussed in this manuscript, manual validation was also employed to remove any further false positives. If the annotations were not due to carry over from natural standards, a molecular ion was observed, the isotopic distribution of the molecular ion and fragments aligned with the proposed formula (especially for compounds containing chlorine), the spectral match and any other evidence clearly showed a top candidate which could be discerned from other candidates, and the peak shape was well defined, the compound was determined to be confirmed manually.

The resulting identifications were aligned and gap filled across samples using a 0.03-min tolerance for alignment. For annotated compounds predicted toxicities were used to highlight compounds of most concern. Predicted toxicity, which included mammalian acute toxicity (rat oral LD_{50}, 24 h) (Zhuet al., 2009), mutagenicity (Sushkoet al., 2010; Benfenati et al., 2009), and developmental toxicity (Cassanoet al., 2010), was estimated using previously developed hierarchical clustering models (Martin et al., 2008) and other models based on molecular structure. Furthermore compounds were classified based on structural motifs using the ClassyFire software (Djoumbou Feunanget al., 2016).

2.3.3. Data filtering to reduce false positives

After peak-picking raw mass spectral data a number of redundant or background features are included which will interfere with statistical analysis. Data filtering and data-workup consists of blank feature filtering (BFF) (Pattersonet al., 2017), removal of duplicate compound identifications, and average score filtering was performed.

The BFF formulas used is shown in Equation 1 Briefly, if the 95th percentile of compound intensities was greater than the average of the blank plus three times the standard deviation, then that feature was retained, otherwise the feature was removed across all samples. The 95th percentile was chosen to retain compounds even if only a few individuals had levels above the “limit of detection” (LOD) as determined in Equation (1) (right hand side). The compound signal intensities were not adjusted using the blank

[1] 1,3,7-Octatriene, 3,7-dimethyl- ((Z)-alpha-Ocimene) is highly correlated with limonene (0.998). The compound is found in green leafy vegetables and pulled out by NMF. Ocimene looks almost identical to the open form of Limonene and therefore (Z)-alpha-Ocimene is likely a miss-annotation and is truly another form of limonene (this is an example of the challenge in discerning nearly identical structural compounds using EI and RI).

intensities. BFF has been shown to improve the number of true positives and decrease the number of false negatives as compared to other filtering techniques (Pattersonet al., 2017; Kirpichet al., 2018). Ideally extraction/field blanks are used which undergo the exact same processes (eg. transport, storage, processing, analysis) as the samples to enable the removal of background contaminants. In this case blanks were let to sit in the freezer for 2 weeks and were prepared in the exact same manner to samples during sample preparation and acquisition. BFF was performed with the following equation:

$$x_{95\%} > (\bar{b} + 3\sigma_b) \quad (1)$$

Where $x_{95\%}$ is the sample 95 percentile, $\bar{b}$ is the blank average, and σ_b is the standard deviation of the blank.

In the case of comparing the most toxic compounds of concern, a more stringent threshold of the 75 percentile being greater than 2x the limit of detection (LOD) was used. Following BFF calculations, redundant molecules were removed (molecules with the same exact name), retaining the molecule with the highest average score from the deconvolution plugin (Thermo). Multiple molecules can exist due to isomers giving the same identification, false positives, or, commonly, improper deconvolution where one peak is considered multiple peaks. Finally, average score filtering was employed. The average score used for filtering was 15.

2.3.4. Targeted peak detection employing MZMine 2

Deconvolution, identification, gap filling, and alignment using the Thermo deconvolution plugin is the computationally expensive part of the data-processing workflow and can crash on larger datasets (eg. the 500+ files used in this study). Therefore, the deconvolution was applied to the first 3 batches in order to determine representative compounds across samples and filtered as discussed above. Following filtering the list of identified compounds across batches was combined, retaining the top average score for a compound if found in multiple batches, and a targeted peak picking list was developed for MZMine (Pluskal et al., 2010). Peak picking is one of the most challenging algorithms to develop in order to reduce false positives, improve true positives, and consistently pick and integrate peaks correctly (Kim and Sim, 2019). Optimal parameters were validated manually using the MZMine visual interface.

The workflow employing MZMine 2.53 (Pluskal et al., 2010) consisted of the following steps:

Raw data import, mass detection (exact mass: minimum intensity − 5000), targeted peak detection (15% intensity tolerance (peak shape), noise level - 10,000, mass tolerance 0.005/5 ppm, and retention time tolerance − 0.04 min), alignment (Join Aligner: mass tolerance 0.01/10 ppm, and retention time tolerance − 0.04 min, weight m/z − 20, weight retention time − 20), and gap-filling (Peak Finder Multicore: intensity tolerance − 10%, mass tolerance 0.01/10 ppm, and retention time tolerance − 0.07 min). The resulting list of peaks was exported as peak heights and TICs were back calculated.

TICs in this case refers to EI deconvoluted spectra and the sum of the fragment intensities to determine the relative amount of a feature across samples. Due to algorithmic error in deconvolution and the increased likelihood of signal overlap from other peaks, TICs are characterized by increased noise as compared to other measures such as reference peak heights and areas. But, the TIC absolute value is useful to compare relative abundances across molecules due to the universality of the EI fragmentation mechanism. Therefore we recalculated TICs (x_{TIC}) from peak heights (x_H) using the ratio of the average TIC ($\bar{x}_{TIC}$) and average peak heights ($\bar{x}_H$) as shown in the following equation:

$$x_{TIC} = x_H \times \frac{\bar{x}_{TIC}}{\bar{x}_H} \quad (2)$$

2.3.5. Quality assurance and quality control (QA/QC)

QA/QC was employed to make sure that:

(1) Any variance in signal intensities of molecular features across acquisition time and batches were determined and corrected;
(2) Features were above the limit of detection (LOD) and not from background signal; and,
(3) The annotation workflow provided accurate identifications (low false positive rate)

Regarding 1), blank samples and neat quality controls (PDMS bars spiked with 71 natural standards) were acquired after every 5 samples. Samples were randomized within and across batches. For all samples, blanks, and quality controls, 12 internal standards were spiked in (Section 2.3). Principal components analysis (PCA) (e.g., Figure S2) and boxplots of compound intensities grouped by batches (e.g., Figure S4) were used to determine batch effects. Molecular feature intensities and internal standard intensities were plotted across acquisition time for each batch to determine trends in intensity versus run order (e.g., Figure S5). No significant trend across run-order was observed for the majority of compounds within batches (spearman rho > 0.05), but significant differences in intensities were observed across batches, likely due to differences in ionization efficiencies after source cleaning procedures performed between batches. Section 2.3.6 below describes batch-wise median normalization, which was developed and applied to correct for this difference in absolute signal across batches.

Regarding 2), BFF was used to remove any features which were attributable to background signal. In addition, stationary passive PDMS samplers deployed (FreshAir Clips) were used to determine personal exposure levels above background atmospheric concentrations. These stationary samplers were placed at different times across all 5 months (see the supplemental Excel file).

Regarding 3), the annotation workflow described in 2.3.2 using Thermo's deconvolution plugin and stringent filtering parameters based on exact mass, retention index, and EI spectral match, was validated against 71 standards. All standards were annotated correctly, or as a close isomer (e.g., 1,3-dichloro-benzene misannotated as 1,2-dichloro-benzene). Those compounds which were hypothesized to have the highest health risk based on predicted toxicities and relative abundances were manually validated (to determine structurally explicit fragments and the molecular ion, screen for similar spectral matches, and look at peak shapes/deconvolution and compare across samples QCs and blanks). Those manually validated and confirmed included: triclosan, dichlorvos, bis(1,3-dichloroisopropyl) ether, triethyl phosphate, 5-methoxy-1,2-dimethylindole, butylated hydroxytoluene, naphthalene, 1,2-benzisothiazole. Those which were false positives were removed (three, QC carryover).

2.3.6. Normalization and statistics

Features were normalized using a novel method introduced here which we term batch-wise median normalization (BMN). BMN is similar to median normalization, which is commonly used in metabolomics (Noonan et al., 2018; Wanget al., 2003). In median normalization a single normalization factor is obtained for each sample and applied across all features (Noonan et al., 2018;

Wanget al., 2003), whereas in BMN a unique normalization factor is calculated for each feature. These normalization factors are calculated to force the median feature intensity for each batch to be equivalent across all batches. In this study samples were grouped into batches, between which the source was cleaned, and the next batch was removed from the freezer. This technique was applied because batch effects were observed which were compound specific, and hence a single normalization factor could not be applied. BMN accounted for any batch-to-batch change in the median compound levels, and since samples were randomized in terms of variables used for statistics, no bias was introduced.

Note that this method has four major assumptions:

(1) That samples within batches are randomly chosen (and hence should have equivalent distributions if no batch effects occurred)
(2) That there are enough samples per batch that the median signal per compound is well characterized and does not vary much by chance (an inaccurate measurement of the median would create a systematic error in intensity throughout the entire batch for that compound)
(3) That variance between batches is simply explained by a discrete increase in each compound between samples in different batches, and in other words, is not dependent on run order or other factors that differ between samples within a batch.
(4) The median is non-zero, and above the limit of detection (Equation 1), which is for the purposes of the 2nd assumption that the median is well characterized.

Compound intensities were checked for variation across run-order, and if no changes were observed then BMN was applied. Following BMN, the data was log transformed (and mean-centered for PCA). PCA and dendrograms for samples colored by batch without and with BMN (Figure S2 and Figure S3) show that BMN removed variance dominated by batch effects. For this dataset variance across the median was similar for BMN compound profiles across batches (Figure S4). The features before (and after) BMN did not trend across run order but rather only by batch (Figure S5), meaning that BMN met assumptions necessary for application.

PCA, PLSDA, ANOVA with Tukey post-hoc test (FDR corrected p-value using Benjamini-Hochberg (Benjamini and Hochberg, 1995) < 0.05), and correlation analysis were employed using MetaboAnalyst (Xia et al., 2015). Spearman's rho (Hamed, 2016) trend analysis across temperature was used to determine the significance of trends in chemicals across outdoor temperature, along with ANOVA across months. R was employed for figures using the beeswarm and ggplot2 (Wickham, 2009) packages. NMF was used to determine six latent variables. Previous papers have shown the advantage of NMF to reduce omics-datasets to interpretable co-correlated components (Yang and Michailidis, 2016; Stein-O'Brienet al., 2018; Béchauxet al., 2013), and specifically for deducing sub-components of mixtures in exposures (Yang and Michailidis, 2016). Latent variables in NMF consist of a vector of weights for all compounds and a vector of weights for all samples. These vectors are optimized in order that when multiplied using the vector outer product and the resulting six matrices are added the experimental data is best approximated. Due to the nature of this optimization (recreating the data only using matrices derived from compound and sample weights) co-correlating features across samples (e.g., from the same chemical source) will be pulled out for each latent variable. Because multiple latent variables are added to recreate the experimental matrix, if a certain compound came from multiple sources, this could be accounted for and the weights to each source may be determined. Note that 6 latent variables were chosen due to six major regions of correlation in the Pearson's correlation matrix organized by Euclidean distance (Fig. 3C).

3. Results and discussion

3.1. Data-processing – compound identification and filtering

The majority of mass spectral features are artifacts or noise (Pattersonet al., 2017; Kirpichet al., 2018); these features can lead to false positives and reduce the statistical power for finding analytes of interest. While over 6000 features across 305 samples (individuals at various time-points and stationary samplers) were annotated and deconvoluted using the Thermo GC deconvolution plugin, 615 higher confidence annotated features were retained (about 10%). These compounds had high spectral match scores, retention indexes within 50 units, and fragment exact masses which could be predicted using only atoms contained in the proposed precursor formula. In addition, these chemicals were unlikely to be contaminated: blank feature filtering was used to remove any compounds which were not above a certain threshold of the blanks (see Section 2.3.3. for exact parameters). Based on manual validation of >20 features of interest and evaluation of the 71 compounds included in the targeted analysis, the only false positives observed were from carryover of spiked standards in quality control (QC) samples and annotation of the wrong isomers for structurally similar compounds.

The use of high resolution (and mass accurate) mass spectrometers can increase both the number and confidence of annotations in gas chromatography mass spectrometry. An example is shown for dichlorvos (Fig. 2), a highly toxic compound found in nearly all individuals which is discussed in Section 3.2.1. Formulas for each fragment (as well as manually hypothesized structures) were able to be predicted; in many cases, only a single reasonable structure could be predicted per fragment with high mass accuracy and 30,000 resolution (Fig. 2A). This structural information provided further confidence in the annotation. High mass accuracy and resolution also improved annotation by discerning fragments from other possible overlapping masses. For example, for *m/z* 184.9764 (Fig. 2A), while only 4 possible formulas could overlap within 5 ppm, 19 formulas could overlap at 30 ppm, and 211 formulas at 500 ppm using the following ranges of possible atoms: $C_{0\text{-}20}H_{0\text{-}40}N_{0\text{-}3}O_{0\text{-}4}P_{0\text{-}1}Cl_{0\text{-}2}S_{0\text{-}1}$. Overlapping masses were also observed experimentally. For most fragments there were a high number of other background masses which fell within 0.1 Da. These fragments often were similar or higher in intensity, and co-eluted with dichlorvos (for example *m/z* 127.0155, Fig. 2C). Furthermore, using unit mass resolution mass spectrometers, dichlorvos would not have been identified in the sample, as the fragment-extracted ion chromatograms could not be deconvoluted from the background signal or signal from other analytes. For example for *m/z* 78.9944 and *m/z* 109.0049 (reference mass), when including signal within about a 1 Da mass range, there were no longer observable peaks (Fig. 2B). The advantage of high mass accuracy and resolution is especially true for the case of our passive sampler analyses were a diverse range of compounds (rich spectra) are measured at relative short chromatographic analyses for higher throughput analysis (less than 30 min of useable chromatographic time).

3.2. Exposure trends and potential sources

3.2.1. Variables leading to the greatest changes in exposure profiles – outdoor temperature

Environmental exposure profiles are dynamic; in order to provide a holistic view of chemical exposure risks, multiple

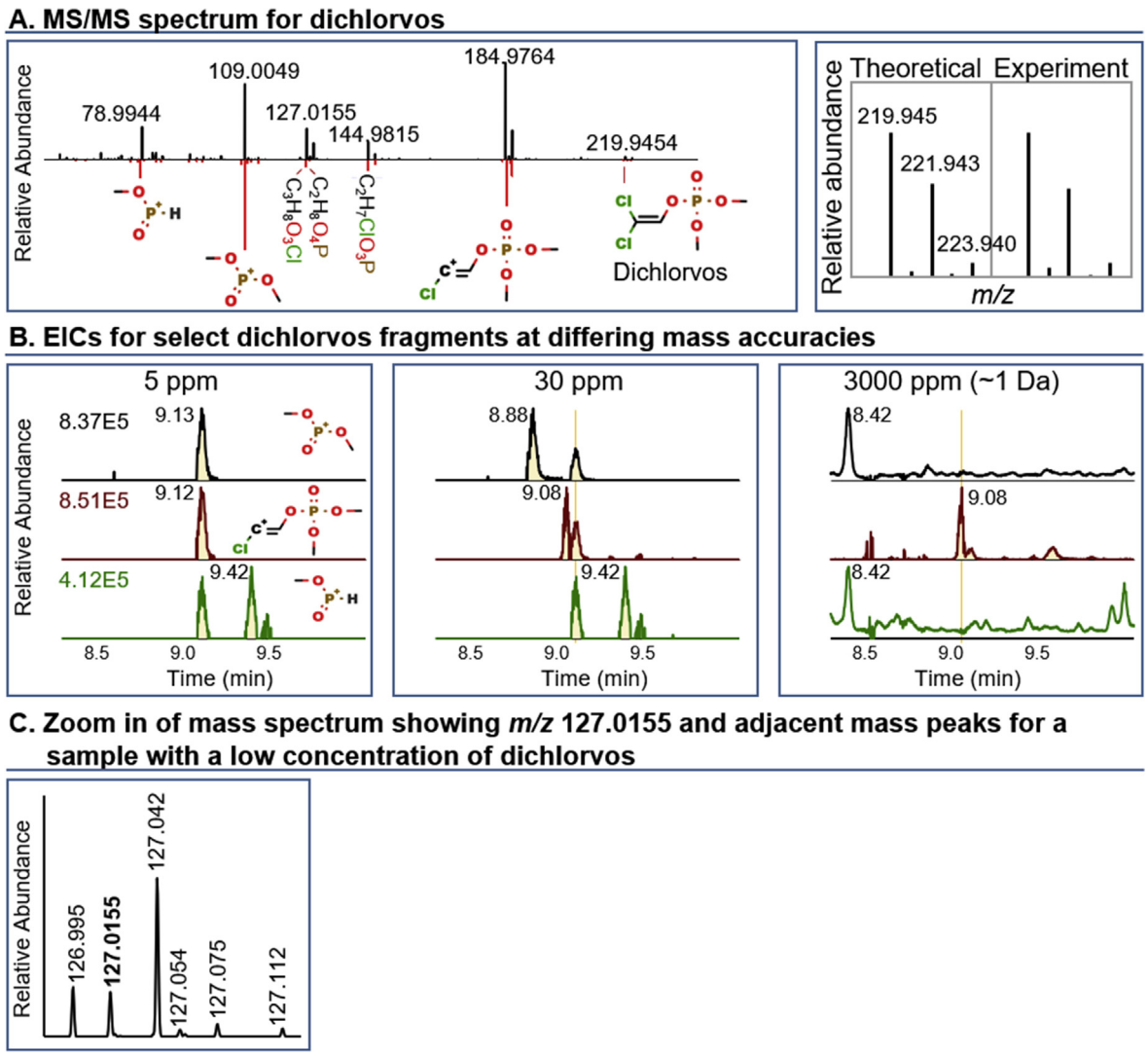

Fig. 2. GC-HRMS electron impact (EI) spectra (A and C) and reconstructed ion chromatograms (EICs) (B) showing the advantage of high resolution and high mass accuracy for identification. The right hand of panel A is a zoom in on the theoretical and experimental isotopic signature of dichlorvos showing high isotopic fidelity. Note that for C, the mass spectrum was for a sample with low levels of dichlorvos to emphasize the advantage of high resolution for the deconvolution of similar masses, whereas in A the spectrum is from a sample with high levels of dichlorvos to emphasize the accurate spectral matching.

measurements across time, individuals, various behaviors, and environments for which individuals' transverse are necessary. The exposure levels of the 615 compounds were often unique across individuals (e.g., Figure S6) and differed across months and outdoor temperature (Figs. 3 and 4, Figure S7, and Figure S9). The greatest variance in exposure profiles was across months; PCA scores plots showed that personal exposure profiles in September were unique as compared to the other months (p-value < 0.0005) and *explained the greatest variance across exposure profiles* (Figure S7). Differences between October and later months explained the second most variance (PC2), whereas all months (November–January) were different in PC3 (p-value < 0.0005). A PCA of variance in exposure profiles against sex showed no major differences between males and females. Hence, minimal variance was explained by comparing individuals when considering all detected compounds (PCA) or compounds individually (t-test, Hochberg corrected). Therefore, variation in temperature was the strongest indicator of differences in exposure profiles in this study. Individual and sex-based differences in exposure profiles may have been partially controlled for due to the tightly controlled nature of the China BAPE study, including activities, diet, and age (Supplemental Information).

Unlike PCA, which calculates scores and loadings based on explanation of total variance, NMF is a factorization method which can determine latent variables, or "parts of a whole" (Lee and Seung, 1999), based on correlating features (Kfouryet al., 2016). In addition, because in NMF multiple latent matrices consisting of the vector outer product of sample and compound weights are summed, and these weights are optimized to best approximate the original experimental data, compounds emitted from multiple sources can be deconvoluted. Although these methods are distinct, NMF chemical weightings were also best explained by temporal changes, further suggesting the dominant role of the change in activity patterns with changing weather on exposure profiles. It is important to note that the number assigned to an NMF pair of participant and compound vector weightings (e.g. NMF 1) is arbitrary; unlike PCA, the components are not ordered by percent explanation of variance.

Of the six vectors of sample weightings generated by NMF, four had the highest weightings corresponding to certain months, which were as follows: one latent variable with high weightings in

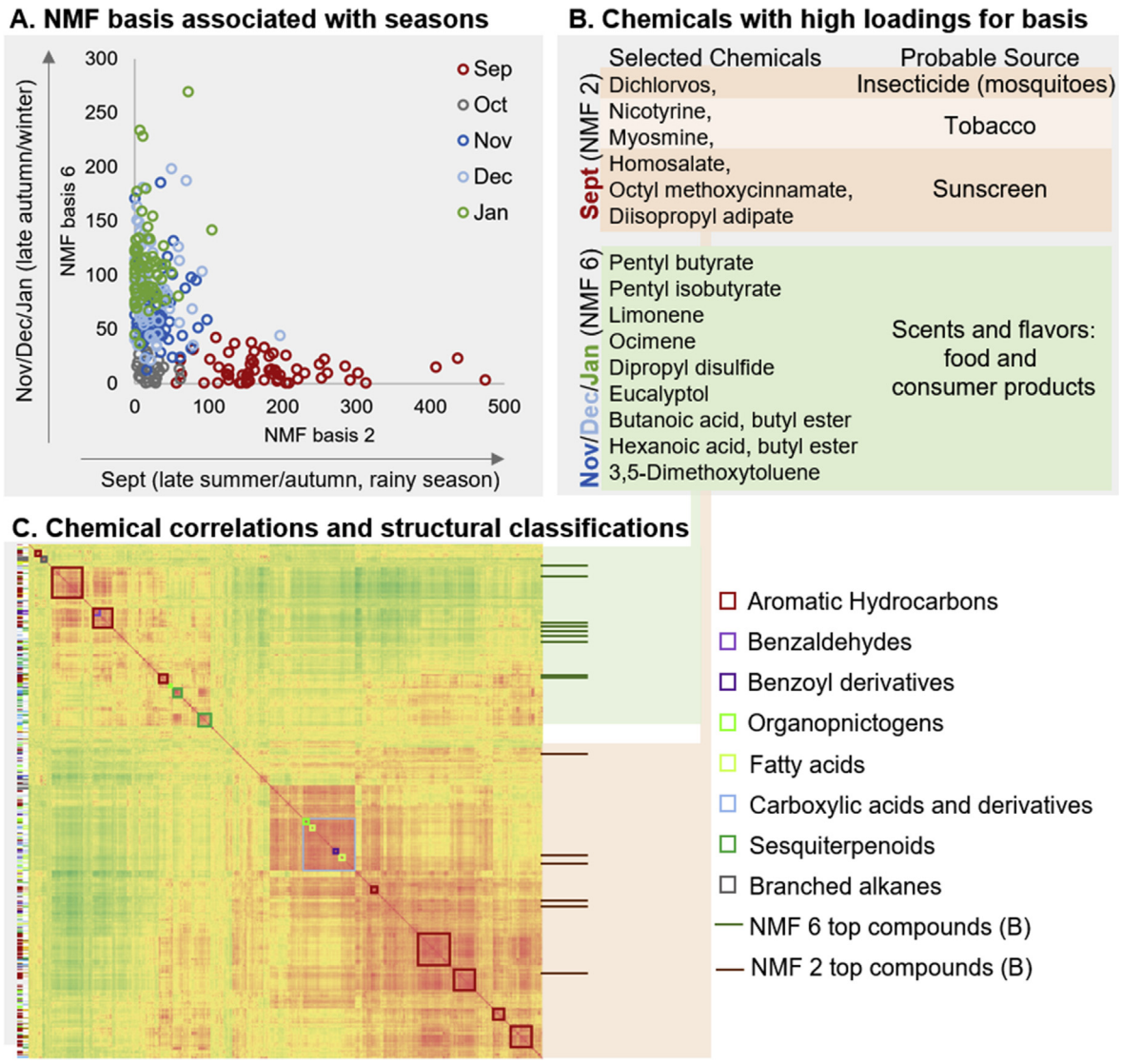

Fig. 3. Determining correlated compounds clusters using non-negative matrix factorization (NMF) (A and B) and a Pearson's correlation matrix (C). One latent variable (NMF basis 2) had samples weights significantly higher in September versus all other months (p-value < 0.0001), whereas NMF basis 6 had sample weights significantly higher in November, December, and January compared to all other sample months (p-value < 0.00001) (A). NMF shows sunscreen compounds (homosolate and octyl methoxycinnamate), pesticide (dichlorvos), and tobacco/cigarette related compounds associated with autumn (September) among many others, and scent and flavoring compounds (all) associated strongly with late autumn and winter months (B). Select compounds (in terms of weights) for these two latent variables are shown in B. For correlation analysis (C) cell color indicates Pearson's correlation (red 1, yellow 0, green -1), and the correlation matrix is organized by Euclidean distance. Bold solid borders indicate 50% or more compounds within a correlation cluster share the same structural classification using Wishart lab's ClassyFire software. Lighter borders (carboxylic acids/derivatives) indicate 25% or more compounds share the same structural classification. A supplementary excel is provided to explore all compounds, classifications, and correlations. (For interpretation of the references to color in this figure legend, the reader is referred to the Web version of this article.)

September, one in October, and two latent variables with higher weights for all of the following three months: November, December, and January (Student t-test p-value < 0.00001 versus other months). This suggests that there are correlating sources of compounds with exposures higher in the late autumn/winter months (November, December, and January) and unique source of compounds highest in September, as well as October. The plot of sample weights for the latent variable with high weights in September against the sample weights for the most significant latent variable for winter (November, December, and January) is shown in Fig. 3A with select top compounds for these latent variables shown in Fig. 3B. The top 19 compound weightings for the four latent variables described above are shown in Table S1B and all weightings are shown in the supplemental excel file.

Trend analysis provided direct evidence of significant and widespread changes in the external exposome corresponding to changes in outdoor temperatures, with 422 (69%) of all 615 personal chemical exposures significantly correlated with temperature readings from the local Jinan station (Spearman Rho p-value < 0.05: supplemental excel). 40% of chemical exposures were found to significantly increase during warmer periods, whereas 29% were found to significantly increase during colder periods (Spearman Rho p-value < 0.05: supplemental excel). These two major clusters of chemical elevated during warm periods and those in cold are also depicted in the correlation matrix (Fig. 3C; red and green highlighting to the right of the matrix, respectively).

Various chemicals released by household activities and consumer products were elevated in the late autumn and winter months (November, December, and January; Fig. 3A). The most significant latent variable (NMF 6) had 80% of the top 15 weighted

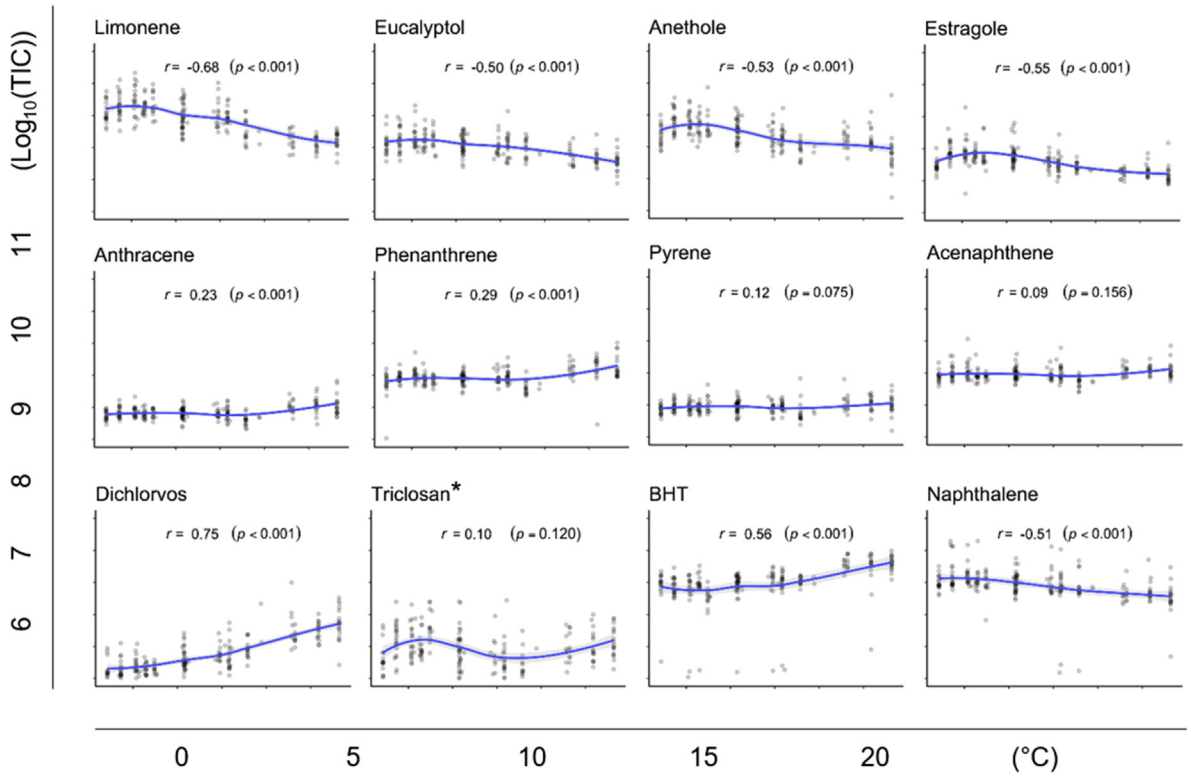

Fig. 4. Variation of select exposures versus temperature. The top set of trends in the log transformed molecular signals (total ion chromatogram, TIC) across temperature are flavoring and aromatic compounds found in food and consumer products, the middle are polycyclic aromatic hydrocarbons (combustion byproducts), and the bottom panel shows a subset of chemicals of potential health concern. Spearman's rank correlation (applied to determine monotonic trends) *r* and *p*-values are shown. Along with temperature compounds followed the same trends (but slightly less significant) with hours of open windows which were correlated with temperature (Figure S20). *The plot of triclosan has the y-axis limit from 4 to 9 instead of 6–11.

compounds consisting of food, flavoring, and scent molecules (Fig. 3B and Table S1A). These molecules included pentyl butyrate (pear or apricot scent found in cigarettes and certain fruits), limonene (highly used lemon scent found in citrus peels and numerous consumer products including cleaners), ocimene (terpene found in a variety of herbs and fruits), dipropyl disulfide (from garlic, onion, and other Allium species), butyl hexanoate (found in fruit and fruit flavorings), 3,5-dimethoxytoluene (major scent compound of roses), and butyl butyrate (pineapple flavor found in many fruits).[1] Overall, 25 sesquiterpenes (plant based molecules), including certain molecules mentioned above, were highly correlated across all participants suggesting common source(s). These sesquiterpenes were determined for a region of chemicals in the Pearson's correlation matrix (Fig. 3C) associated with NMF 6 (November, December, and January).

The significant number of chemicals from food, consumer products, and indoor sources identified during the late autumn and winter months is likely due to the increase in closed windows during these months (Zhouet al., 2020) (Figure S9), which can lead to an accumulation of compounds in the indoor environment (Howard-Reed et al., 2002; Ghosh et al., 2013; Date, 2017). Absolute levels of these food flavoring and scent molecules were found to significantly increase during colder weather (four examples shown in Fig. 4 and Figure S8, top four plots) and with longer hours of closed windows (Figure S10). For example, limonene (likely from cleaning) increased dramatically (nearly 2 orders of magnitude) from the hottest to coldest months (Fig. 4 and Figure S8). These molecules could potentially be used to determine meta-data on participants, including when and how much participants cleaned, what products they used, what participants' diets contained, and which participants cooked. It is currently challenging to assess diet sources using questionnaires; we show that personal exposure profiles of food molecules measured using personal passive samplers may be helpful for discerning components of diet down to the resolution of food additives.

For the latent variable (NMF 2) associated with September, the warmest month (average temp = 21.9 ± 2.4 °C as compared to the coldest month, January: 0.2 ± 1.7 °C) in this study, the top five identified compounds included two chemicals commonly found in sunscreen (homosolate and octyl methoxycinnamate) and one chemical that has been a popular insecticide in the study region (dichlorvos for malaria control) (Figs. 3B and 4, and Table S1B). Compounds frequently associated with vehicle tailpipe and coal-related emissions (山东济南四大大气污染源分布大剖析 - 北极星环保网) were also highly weighted (e.g. xylene and m-cresol), as well as cigarette related compounds (nicotyrene and myosmine) (Fig. 3B and Table S1B). Outdoor exposure during September based on windows being open more (Figure S9) as well as direct use of certain chemicals in this warmer month, such as dichlorvos and sunscreen, are likely the main reasons for the stark contrasts in early autumn profiles (September) as compared to winter.

This manuscript is one of the first to show the advantages of NMF in determining sub-components of complex exposure mixtures and associated patterns across individuals.

3.3. Screening for chemicals of concern

By using predictive models of toxicity (Zhuet al., 2009; Sushkoet al., 2010; Benfenati et al., 2009; Cassanoet al., 2010; Martin et al., 2008; Kwiecienet al., 2015), we were able to

determine which compounds might pose the most risk to the health of study participants. It is important to note that certain toxic endpoints (e.g. reproductive toxicity) were not discussed, that certain compounds not contained in the EPA ChemDashboard database (23%) did not have predicted toxicities assigned, and that relative exposure levels could vary depending on partition coefficients and other compound-specific factors influencing signal intensity. While this method for prioritizing chemical compounds is incomplete, it provides top chemicals of concern which should be investigated further. The top 5 mutagenic compounds were benzenamine, 2-chloro-4,6-dinitro-, cyclopenta[cd]pyrene, TCPP, 1-methyl-pyrene, and 6-methlyl-quinoline, while the top 5 compounds in terms of developmental toxicity were linderol, m-cresol, dehydroabietic acid, 9H-fluorene, 2-ethylcyclohex-2-en-1-ol, and 2-menthene. In terms of mammalian acute toxicity, the top 5 most toxic compounds detected after manual validation of annotations in order of rat LD50s (smallest to largest) were triclosan, dichlorvos, bis(1,3-dichloroisopropyl) ether, triethyl phosphate, and 5-methoxy-1,2-dimethylindole (Fig. 5A). It is interesting to note that the top 3 acutely toxic compounds were all chlorinated species. By accounting for the relative intensity of the compounds (multiplying a compounds total ion chromatogram (TIC) by the inverse of the rat LD50), the top 5 compounds of concern were dichlorvos, butylated hydroxytoluene, naphthalene, bis(1,3-dichloroisopropyl) ether, and 1,2-benzisothiazole, respectively (Fig. 2B). All EI spectra and chromatograms were manually validated for these potentially high-risk compounds.

Using EI, the total deconvoluted spectra is often representative of relative abundances between compounds (EI is a universal ionization mechanism) allowing for screening the most abundant and toxic compounds. But, in the case of passive samplers, it is important to note that differences in uptake linear ranges depend on the passive sampler-air partition coefficient and will influence the total signal obtained (Lin et al., 2020; Shoeib and Harner, 2002). Modeling uptake rates of chemicals into PDMS has previously been performed to better estimate airborne concentrations (Okemeet al., 2018), and further work validating this for our sampler with our unique wearable form factor will be done to better link the dose to

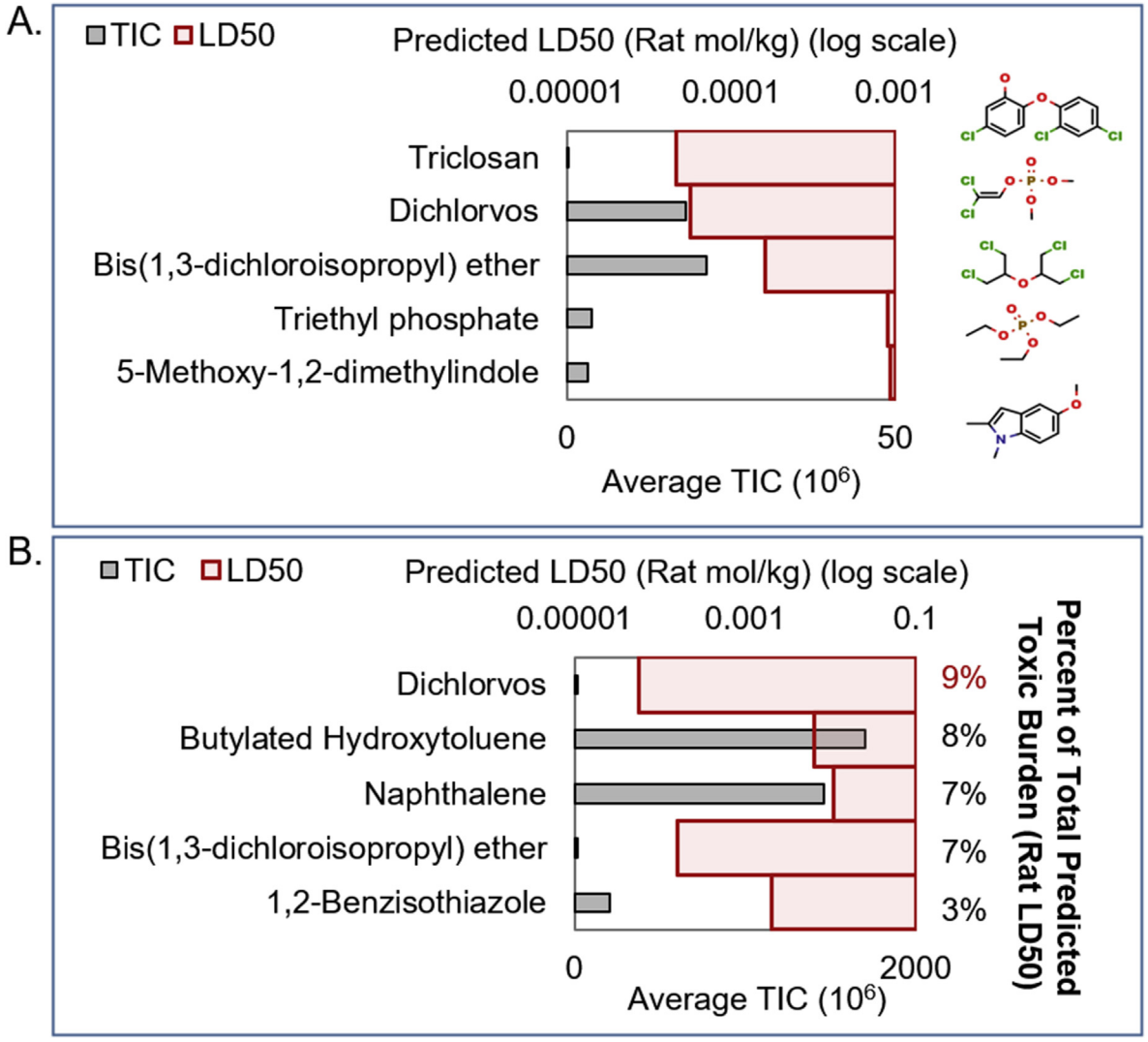

Fig. 5. Predicted toxicities (oral rat 24-h 50% lethal dose) ranked by predicted toxicity alone (A), and predicted toxicity weighted by relative abundance (B). Percent of total predicted toxic burden, is the total ion chromatogram (TIC) average signal across samples (minus blank signal) multiplied by the reciprocal of the value of the predicted toxicity as a percentage of value across all compounds. In this case, TIC refers to the summed signal from all observed fragments. In EI ionization is universal, the chemistry of a compound minimally effects the TIC abundance, unlike in liquid chromatography, and hence can be used to compare relative levels of chemicals. Limitations of using TIC as a measure of abundance using passive samplers is described in-depth in Section 3.2.

toxicity of compounds to screen for compounds of most concern.

3.3.1. Exposures of potential concern – compounds and likely sources

For designing future interventions, it is important to know both which chemicals pose the greatest health risks, and their likely emission sources. Using wearable passive samplers, hundreds of chemical exposures were measured. In a subset of cases, we were able to narrow the suspect sources to a single likely source. These were cases when the chemical was used in one dominant use (e.g. dichlorvos and homosalate). Hence, integration of additional libraries detailing source profiles is needed to link exposures to specific emissions.

3.3.1.1. Dichlorvos – widespread insecticide exposure. Dichlorvos was of greatest concern using current approaches based on high acute toxicity and relatively high signals detected in the passive wristband samplers (Fig. 5). Dichlorvos is a neurotoxin which is toxic upon inhalation, dermal exposure, and ingestion, which can lead to death, genotoxic, neurological, reproductive, carcinogenic, immunological, hepatic, renal, respiratory, metabolic, and dermal effects (Okoroiwu and Iwara, 2018). For this reason, dichlorvos is banned in many countries including Europe, and restricted in the United States. Dichlorvos is a biocide used for insect control (indoors), grains and livestock. Detection of dichlorvos in the Yellow River, which runs through the Jinan province, has been found to be highest compared to other water bodies in China and dichlorvos was the most commonly detected organophosphorus pesticide in these water bodies (Gaoet al., 2009). Dichlorvos is used during wet and warm seasons in China, where it is directly applied to the indoor environment (including households) via fumigation/spraying mainly for mosquito control. The use of dichlorvos in China is widespread, which is reflected in mosquito and housefly populations evolving resistance to the pesticide (Cuiet al., 2006a; Cuiet al., 2006b; Liet al., 2016; MeiQinget al., 2013). The use of dichlorvos in the study population was confirmed by field personnel.

The use of dichlorvos to control mosquitos (a vector for malaria) is reflected in trends across changes in outdoor temperature measured in this study (Fig. 4, bottom left). Personal exposure levels of dichlorvos significantly decreased (Spearman $r = 0.75$, $p < 0.001$) in colder weather (Fig. 4). Average personal exposure levels in September were 4-fold, 10-fold, and 30-fold higher than in October, November and December, respectively (Figure S8). These patterns reflect the use during warming weather as an insecticide, and use in the indoor environment is emphasized by the much higher levels for personal exposures (wristbands) as compared to stationary outdoor measurements (Figure S8).

While females have generally been reported to apply the mosquito repellant, there was no significant difference in dichlorvos levels based on sex (Figure S8). This is likely attributable to the elderly cohort studied, public rather than private application of dichorvos, or return of all members to the household after application (dichlorvos takes 3–6 h to break down) (R - Public Health Sta, 2020). Dichlorvos exposures varied widely, with one individual having levels 29-fold higher than median levels in September. Pesticide poisoning in China is relatively high, with dichlorvos being one of the most common causes of mortality from acute pesticide exposure (Yimaeret al., 2017; Wanget al., 2019b). Based on our results, passive sampling monitoring may be used to determine if, and when, an individual may be exposed to high levels of pesticides, providing information for interventions to reduce risks of pesticide exposure on both the community and individual level.

3.3.1.2. Chemicals from preservatives and soaps. Two molecules of concern from an acute exposure standpoint were BHT, an antioxidant used in everything from food to rubber, and triclosan, a chemical with anti-microbial, anti-viral, and anti-fungal properties used for example in certain soaps and hand sanitizers (Fig. 5). Monthly variations show BHT exposure is significantly higher in the warmer and wetter month of September compared to later months (Fig. 4), but higher in personal samplers as compared to stationary sampler (Figure S8). Because of the prevalence of BHT in a number of consumer, food, and industrial products it is difficult to hypothesize the source of BHT without further studies. While BHT is generally considered safe due to low dermal absorption (Lanigan and Yamarik, 2002), measurement in passive samplers indicated a significant inhalation route of exposure which warrants further health studies. For triclosan, which can cause mitochondrial dysfunction, current data suggests health risks even at levels for which people are often exposed (Weatherly and Gosse, 2017). Furthermore, similar to BHT, the chemical toxicity has primarily been determined through oral and dermal intake, and further work on toxicity when inhaled is needed.

3.3.1.3. Naphthalene – unique indoor sources of PAHs. Naphthalene personal exposure was found to increase in our study population during the winter months (Fig. 4). In a study in Hangzhou, China, naphthalene was the highest detected PAH in the indoor environment and about 75% of naphthalene in non-smoking households came from mothballs (Zhu et al., 2009). With the major sink for naphthalene being the outdoor environment (Zhu et al., 2009), the increase in naphthalene exposure in winter is likely due decreased outdoor ventilation in participants' homes. Trends across months suggest a major source of indoor naphthalene exposure is mothballs, especially given that tobacco related chemicals were elevated in the warmer month of September, as opposed to winter months when Naphthalene levels peaked (Fig. 3B). High levels of naphthalene measured in stationary samplers (averages equivalent to the December and January personal exposure levels; Figure S8) suggest another contributor is vehicle tailpipe emissions, coal combustion, and/or other combustion products in the outdoor environment (Jia and Batterman, 2010).

3.3.1.4. PAH exposure – numerous indoor and outdoor sources discerned from personal exposure monitoring. In terms of individual PAHs, only naphthalene was a top contributor to estimated toxic burden (Fig. 5); when accounting for their combined emissions, individual sources of cumulative PAH exposure may be as or more toxic then individual compounds. Using correlation analysis, 183 compounds, consisting of mainly aromatic and polycyclic aromatic compounds, were identified to form nine clusters (Fig. 3C; with cluster's average Pearson's coefficient of 0.71). These compounds mainly consisted of naphthalene derivatives, fluorine derivatives, biphenyls and derivatives, phenanthrene and derivatives, anthracene and derivatives, and benzene and derivatives (supplemental excel).

Five correlated clusters (Fig. 3C, bottom right) of 108 PAHs were associated with the warmer month of September based on NMF compound weightings (Fig. 3) and trend analysis (Supplemental Excel), with aromatic hydrocarbons also showing up as the highest percentage (28%) of molecules with significant and robust correlations using network analysis (Figure S11). Higher levels during warmer weather, when more cumulative time was spent outdoors (Figure S9) and with participant's windows open (Fig. 4, Figure S8, Figure S9, and Figure S10), suggests predominant exposure from the outdoor environment. In addition, relatively high levels of certain PAHs in these clusters in stationary outdoor samplers, such as anthracene and phenanthrene (Figure S8), were observed. Possible PAH contributors are vehicle tailpipe emissions, coal

combustion, and other combustion products in the outdoor environment (Jia and Batterman, 2010). These five clusters of 108 PAHs associated with warmer weather (September) and high in outdoor monitors (Fig. 3C, bottom right), are likely decreased in winter months due to participants spending less time outside and having windows closed more often (Figure S9).

The remaining four correlated clusters of 75 PAHs (Fig. 3C, top left) were associated with colder winter months where participants would spend more time indoors based on NMF analysis (Fig. 3). These aromatic hydrocarbons were likely primarily derived from indoor sources. These compounds also correlated with chemicals expected to be from indoor sources: common compounds found in household cleaning products such as limonene, PAHs such as naphthalene, likely from mothballs (Zhu et al., 2009) (Fig. 4), and terpenes, which are likely from cooking meat (Chevanceet al., 2000) and vegetables (Chizzola et al., 2013) (Fig. 3C). The compounds were generally higher in the colder months when windows were closed. Therefore, passive samplers and correlation analysis may distinguish unique sources of both indoor and outdoor PAHs and aromatic hydrocarbons.

4. Conclusions

Environmental exposures are a leading risk factor for disease and mortality globally, and yet the following questions remain: what are our personal exposure profiles and how do they change overtime, how toxic are these chemicals, and what are the sources of these exposures? We were able to address all three questions by measuring personal exposure profiles using wearable passive samplers across seventy-six healthy Chinese elderly participants longitudinally over five months. Using a novel gas chromatography mass spectrometry workflow which increased throughput, allowed for the analysis of large cohort studies, and increased accuracy of annotations, we were able to tentatively identify 615 different chemical exposures. This list included chemical exposures to substances banned in several countries due to toxicity, and yet these chemicals were prevalent across the population.

Using factorization techniques and multivariate analysis, exposure profiles were found to be most influenced by changes in weather, with the warmer wetter months different from the dryer colder months. Increased exposures during warm periods included chemicals in sunscreens and cigarettes, insecticide exposure, and increased exposures to 108 aromatic and polyaromatic hydrocarbons. Winter exposures were dominated by chemicals from fragrance and flavoring compounds in food and consumer products which likely increased due to lower ventilation (more hours of closed windows). Chemicals of concern included dichlorvos from indoor and (and potentially outdoor) spraying for mosquito control, naphthalene, with a dominant source likely being mothballs, and combustion products from multiple sources.

While this study was able to evaluate exposure differences between warmer and cooler periods, future studies spanning an entire year, or ideally multiple years, are needed to better understand seasonal trends in environmental chemical exposures. Furthermore, this paper focused on a subgroup of the Chinese population who were all similarly age and lived in the same city. Studies evaluating a larger number and more diverse group of participants (age, ethnicity/race, geography) are needed for determining the risk profiles of the population at large. Our wristband technology has been deployed internationally with a broad range of populations. Compilation exposures across these varied populations could provide even broader understanding of global exposure dynamics.

By developing personal exposure monitoring technology, high-throughput software for analysis, and statistics to discern exposure characteristics and sources, this work sets a precedent for linking our environmental exposures and health.

Credit author statement

Jeremy Koelmel: Conceptualization; Data curation; Formal analysis; Investigation; Methodology; Project administration; Software; Supervision; Validation; Visualization; Roles/Writing - original draft; Writing - review & editing. Elizabeth Lin: Conceptualization; Data curation; Investigation; Methodology; Project administration; Supervision; Roles/Writing - original draft; Writing - review & editing. Pengfei Guo: Data curation; Formal analysis; Visualization; Writing - review & editing. Jieqiong Zhou: Data curation; Project administration; Writing - review & editing. Jucong He: Software; Writing - review & editing. Alex Chen: Software; Writing - review & editing. Chris Beecher: Conceptualization; Software; Writing - review & editing. Ying Gao: Investigation; Data curation. Fuchang Deng: Investigation; Data curation. Haoran Dong: Investigation; Data curation. Yuanyuan Liu: Investigation; Data curation. Yu'e Cha: Investigation; Data curation. Jianlong Fang: Investigation; Data curation; Project administration. Song Tang: Conceptualization; Data curation; Funding acquisition; Investigation; Methodology; Project administration; Resources; Writing - review & editing. Xiaoming Shi: Conceptualization; Data curation; Funding acquisition; Investigation; Methodology; Project administration; Resources; Writing - review & editing. Krystal J. Godri Pollitt: Conceptualization; Funding acquisition; Investigation; Methodology; Project administration; Resources; Supervision; Visualization; Roles/Writing - original draft; Writing - review & editing.

Declaration of competing interest

The authors declare that they have no known competing financial interests or personal relationships that could have appeared to influence the work reported in this paper.

Acknowledgments

We gratefully thank the National Research Program for Key Issues in Air Pollution Control (No. DQGG0401) to Prof. Shi. We gratefully thank all the participants of Panel Study, Dianliu Community, Ankang Community Hospital, Jinan Center for Disease Control and Prevention, and Shandong Center for Disease Control and Prevention. The present findings and conclusions are those of the authors and have not been subjected to the peer and policy review from China CDC and therefore does not necessarily reflect the views of the China CDC and no official endorsement should be inferred.

Appendix A. Supplementary data

Supplementary data to this article can be found online at https://doi.org/10.1016/j.envpol.2020.116228.

References

Aksenov, A.A., et al., 2020. Algorithmic Learning for Auto-Deconvolution of GC-MS Data to Enable Molecular Networking within GNPS. bioRxiv, 0vol. 1.13.905091 (2020).
Béchaux, C., et al., 2013. Identification of pesticide mixtures and connection between combined exposure and diet. Food Chem. Toxicol. 59, 191–198.
Benfenati, E., et al., 2009. Predictive models for carcinogenicity and mutagenicity: frameworks, state-of-the-art, and perspectives. J. Environ. Sci. Health Part C 27, 57–90.
Benjamini, Y., Hochberg, Y., 1995. Controlling the false discovery rate: a practical and powerful approach to multiple testing. J. Roy. Stat. Soc. B 57, 289–300.

Breysse, P.N., et al., 2010. Indoor air pollution and asthma in children. Proc. Am. Thorac. Soc. 7, 102–106.
Cassano, A., et al., 2010. CAESAR models for developmental toxicity. Chem. Cent. J. 4, S4.
Cassee, F.R., Héroux, M.-E., Gerlofs-Nijland, M.E., Kelly, F.J., 2013. Particulate matter beyond mass: recent health evidence on the role of fractions, chemical constituents and sources of emission. Inhal. Toxicol. 25, 802–812.
Chevance, F.F.V., et al., 2000. Effect of some fat replacers on the release of volatile aroma compounds from low-fat meat products. J. Agric. Food Chem. 48, 3476–3484.
Chizzola, R., 2013. Regular monoterpenes and sesquiterpenes (essential oils). In: Ramawat, K.G., Mérillon, J.-M. (Eds.), Natural Products: Phytochemistry, Botany and Metabolism of Alkaloids, Phenolics and Terpenes. Springer, pp. 2973–3008.
Choi, J., Knudsen, L.E., Mizrak, S., Joas, A., 2017. Identification of exposure to environmental chemicals in children and older adults using human biomonitoring data sorted by age: results from a literature review. Int. J. Hyg Environ. Health 220, 282–298.
Cui, F., et al., 2006. Insecticide resistance in Chinese populations of the Culex pipiens complex through esterase overproduction. Entomol. Exp. Appl. 120, 211–220.
Cui, F., et al., 2006. Recent emergence of insensitive acetylcholinesterase in Chinese populations of the mosquito Culex pipiens (Diptera: Culicidae). J. Med. Entomol. 43, 878–883.
Date, G., 2017. Towards a Better Understanding of Indoor Exposure to Air Pollutants: Window Opening Occurrence in U.S. Residences. Masters Theses.
Djoumbou Feunang, Y., et al., 2016. ClassyFire: automated chemical classification with a comprehensive, computable taxonomy. J. Cheminf. 8, 61.
Gao, J., et al., 2009. The occurrence and spatial distribution of organophosphorous pesticides in Chinese surface water. Bull. Environ. Contam. Toxicol. 82, 223–229.
Gao, Dong, Ripley, Susannah, Weichenthal, Scott, Godri Pollitt, Krystal, 2020. Ambient particulate matter oxidative potential: Chemical determinants, associated health effects, and strategies for risk management. Free Radical Biology and Medicine 151, 7–25.
Ghosh, J.K.C., Wilhelm, M., Ritz, B., 2013. Effects of residential indoor air quality and household ventilation on preterm birth and term low birth weight in Los angeles county, California. Am. J. Publ. Health 103, 686–694.
Guan, W.-J., Zheng, X.-Y., Chung, K.F., Zhong, N.-S., 2016. Impact of air pollution on the burden of chronic respiratory diseases in China: time for urgent action. Lancet 388, 1939–1951.
Hamed, K.H., 2016. The distribution of Spearman's rho trend statistic for persistent hydrologic data. Hydrol. Sci. J. 61, 214–223.
Hammel, S.C., Hoffman, K., Webster, T.F., Anderson, K.A., Stapleton, H.M., 2016. Measuring personal exposure to organophosphate flame retardants using silicone wristbands and hand wipes. Environ. Sci. Technol. 50, 4483–4491.
Hammel, S.C., Phillips, A.L., Hoffman, K., Stapleton, H.M., 2018. Evaluating the use of silicone wristbands to measure personal exposure to brominated flame retardants. Environ. Sci. Technol. 52, 11875–11885.
Howard-Reed, C., Wallace, L.A., Ott, W.R., 2002. The effect of opening windows on air change rates in two homes. J. Air Waste Manag. Assoc. 52, 147–159.
Jia, C., Batterman, S., 2010. A critical review of naphthalene sources and exposures relevant to indoor and outdoor air. Int. J. Environ. Res. Publ. Health 7, 2903–2939.
Kelly, F.J., Fussell, J.C., 2012. Size, source and chemical composition as determinants of toxicity attributable to ambient particulate matter. Atmos. Environ. 60, 504–526.
Kfoury, A., et al., 2016. PM2.5 source apportionment in a French urban coastal site under steelworks emission influences using constrained non-negative matrix factorization receptor model. J. Environ. Sci. 40, 114–128.
Kim, H., Sim, S.-H., 2019. Automated peak picking using region-based convolutional neural network for operational modal analysis. Struct. Contr. Health Monit. 26, e2436.
Kirpich, A.S., et al., 2018. SECIMTools: a suite of metabolomics data analysis tools. BMC Bioinf. 19.
Kwiecien, N.W., et al., 2015. High-resolution filtering for improved small molecule identification via GC/MS. Anal. Chem. 87, 8328–8335.
Lanigan, R.S., Yamarik, T.A., 2002. Final report on the safety assessment of BHT(1). Int. J. Toxicol. 21 (Suppl. 2), 19–94.
Lee, D.D., Seung, H.S., 1999. Learning the parts of objects by non-negative matrix factorization. Nature 401, 788–791.
Li, C., et al., 2016. Identification of genes involved in pyrethroid-, propoxur-, and dichlorvos- insecticides resistance in the mosquitoes, Culex pipiens complex (Diptera: Culicidae). Acta Trop. 157, 84–95.
Lin, E.Z., Esenther, S., Mascelloni, M., Irfan, F., Godri Pollitt, K.J., 2020. The fresh air wristband: a wearable air pollutant sampler. Environ. Sci. Technol. Lett. https://doi.org/10.1021/acs.estlett.9b00800 (March 17, 2020).
Martin, T.M., Harten, P., Venkatapathy, R., Das, S., Young, D.M., 2008. A hierarchical clustering methodology for the estimation of toxicity. Toxicol. Mech. Methods 18, 251–266.
MeiQing, L., et al., 2013. Seasonal variation in population density, dengue virus carriage, and dichlorvos resistance of Aedes albopictus in urban and rural areas of Guangzhou city, China. Zhongguo Meijie Shengwuxue ji Kongzhi Zazhi = Chin. J. Vector Biol. Contr. 24, 108–111.
Noonan, M.J., Tinnesand, H.V., Buesching, C.D., 2018. Normalizing gas-chromatography–mass spectrometry data: method choice can alter biological inference. Bioessays 40, 1700210.
Okeme, J.O., et al., 2018. Passive air sampling of flame retardants and plasticizers in Canadian homes using PDMS, XAD-coated PDMS and PUF samplers. Environ. Pollut. 239, 109–117.
Okoroiwu, H.U., Iwara, I.A., 2018. Dichlorvos toxicity: a public health perspective. Interdiscipl. Toxicol. 11, 129–137.
O'Connell, S.G., Kincl, L.D., Anderson, K.A., 2014. Silicone wristbands as personal passive samplers. Environ. Sci. Technol. 48, 3327–3335.
Patterson, R.E., et al., 2017. Improved experimental data processing for UHPLC–HRMS/MS lipidomics applied to nonalcoholic fatty liver disease. Metabolomics 13, 142.
Pluskal, T., Castillo, S., Villar-Briones, A., Orešič, M., 2010. MZmine 2: modular framework for processing, visualizing, and analyzing mass spectrometry-based molecular profile data. BMC Bioinf. 11, 395.
Prüss-Üstün, A., et al., 2016. Preventing Disease through Healthy Environments: A Global Assessment of the Burden of Disease from Environmental Risks. World Health Organization.
ATSDR, April 26, 2020. Public Health Statement: Dichlorvos.
Rappaport, S.M., 2016. Genetic factors are not the major causes of chronic diseases. PloS One 11, e0154387.
Seethapathy, S., Górecki, T., Li, X., 2008. Passive sampling in environmental analysis. J. Chromatogr. A 1184, 234–253.
Shoeib, M., Harner, T., 2002. Characterization and comparison of three passive air samplers for persistent organic pollutants. Environ. Sci. Technol. 36, 4142–4151.
Stein-O'Brien, G.L., et al., 2018. Enter the matrix: factorization uncovers knowledge from omics. Trends Genet. 34, 790–805.
Sushko, I., et al., 2010. Applicability domains for classification problems: benchmarking of distance to models for Ames mutagenicity set. J. Chem. Inf. Model. 50, 2094–2111.
Wang, W., et al., 2003. Quantification of proteins and metabolites by mass spectrometry without isotopic labeling or spiked standards. Anal. Chem. 75, 4818–4826.
Wang, S., et al., 2019. Silicone wristbands integrate dermal and inhalation exposures to semi-volatile organic compounds (SVOCs). Environ. Int. 132, 105104.
Wang, N., et al., 2019. Epidemiological characteristics of pesticide poisoning in Jiangsu Province, China, from 2007 to 2016. Sci. Rep. 9, 1–8.
Weatherly, L.M., Gosse, J.A., 2017. Triclosan exposure, transformation, and human health effects. J. Toxicol. Environ. Health B Crit. Rev. 20, 447–469.
Wheelock, C.E., Rappaport, S.M., 2020. The role of gene–environment interactions in lung disease: the urgent need for the exposome. Eur. Respir. J. 55.
Wickham, H., 2009. ggplot2: Elegant Graphics for Data Analysis. Springer-Verlag. https://doi.org/10.1007/978-0-387-98141-3 (April 27, 2020).
Wild, C.P., 2005. Complementing the genome with an "exposome": the outstanding challenge of environmental exposure measurement in molecular epidemiology. Canc. Epidemiol. Biomarkers Prev. 14, 1847–1850.
Xia, J., Sinelnikov, I.V., Han, B., Wishart, D.S., 2015. MetaboAnalyst 3.0—making Metabolomics More Meaningful. Nucl. Acids Res., p. gkv380
Yang, Z., Michailidis, G., 2016. A non-negative matrix factorization method for detecting modules in heterogeneous omics multi-modal data. Bioinformatics 32, 1–8.
Yimaer, A., et al., 2017. Childhood pesticide poisoning in Zhejiang, China: a retrospective analysis from 2006 to 2015. BMC Publ. Health 17.
Zhang, D., et al., 2010. The assessment of health damage caused by air pollution and its implication for policy making in Taiyuan, Shanxi, China. Energy Pol. 38, 491–502.
Zhang, X., et al., 2013. Effect of wind on the chemical uptake kinetics of a passive air sampler. Environ. Sci. Technol. 47, 7868–7875.
Zhou, H., et al., 2020. Personal black carbon exposure and its determinants among elderly adults in urban China. Environ. Int. 138, 105607.
Zhu, L., Lu, H., Chen, S., Amagai, T., 2009. Pollution level, phase distribution and source analysis of polycyclic aromatic hydrocarbons in residential air in Hangzhou, China. J. Hazard Mater. 162, 1165–1170.
Zhu, H., et al., 2009. QSAR modeling of rat acute toxicity by oral exposure. Chem. Res. Toxicol. 22, 1913–1921.
山东济南四大大气污染源分布大剖析 - 北极星环保网 (June 5, 2020).